Turkish Journal of Electrical Engineering & Computer Sciences

http://journals.tubitak.gov.tr/elektrik/

Research Article

Turk J Elec Eng & Comp Sci
(2017) 25: 1680 – 1692

doi:10.3906/elk-1509-72

Research on magnetic field state analysis of a nonsalient pole synchronous generator

Baojun GE, Pin LV*, Dajun TAO, Fang XIAO, Hongsen ZHAO
College of Electrical and Electronic Engineering, Harbin University of Science and Technology, Harbin, China

Received: 10.09.2015 • **Accepted/Published Online:** 10.06.2016 • **Final Version:** 29.05.2017

Abstract: This paper is based on the definition of minor asymmetric degree and the relative position of the magnetic field. The relative position of the magnetic field is the angle between the positive and negative sequence magnetic fields. The corresponding relationship between the nonsalient pole synchronous generator steady performance and the magnetic field state is discussed when the generator operates at minor asymmetry. To analyze this corresponding relationship, the Taylor expansion formula with Lagrange remainder and symmetrical components is adopted. We study the relationship between the armature current and the relative position of the magnetic field, deducing the armature current expressions with second-order remainders. The law of the armature voltage is also obtained by phasor analysis. As an example, this paper executes two-dimensional finite element numerical calculations on a nonsalient pole synchronous generator. The result shows that the numerical calculation agrees with the deduced expression, which verifies the correctness of the expressions. In the meantime, during the process of deducing the expressions, a method of calculating the positive and negative sequence currents is proposed and their effective range is offered. When the generator works at maximum overvoltage and maximum undervoltage, the specific value of the relative position of the magnetic field is presented. This paper has important implications for generator running and protection.

Key words: Minor degree of asymmetry, relative position of the magnetic field, nonsalient pole synchronous generator, positive sequence current, negative sequence current

1. Introduction

The nonsalient pole synchronous generator is important power supply equipment in the power system. When the generator works with asymmetric load, the armature voltage and the armature current become unbalanced. Normally, the finite element numerical calculation method has been adopted to solve these asymmetric problems [1–4]. This method has been employed to analyze the magnetic field's state and distortion [5–8]. However, the theoretical analysis of the magnetic field state has been limited to the symmetrical state [9–11]. The magnetic field distortion in DC and AC machines was discussed in [12–14]. This paper investigates the magnetic field state under asymmetrical conditions. The magnetic field has been divided into the positive sequence magnetic field and negative sequence magnetic field [15–18]. The above works have only investigated the symmetrical magnetic field state. The theoretical method in this paper expands the scope of the theoretical analysis of the magnetic field. It has theoretical innovation, and it can also provide valuable expertise for generator protection.

Based on the research of the magnetic field state in this paper, a new method for the stator positive and stator negative sequence currents is proposed. Even the error of this method is given by a precise numerical

*Correspondence: lvpinhrbust@163.com

value. Compared to the old methods, which require large scales of power electronics, this new method can save money and is easily accessible [19–23]. Moreover, regarding the error, in the low asymmetrical degree the method discussed in this paper has more accurate value. However, in the high asymmetrical degree the former method has a more accurate value.

The overvoltage and undervoltage faults in generators have produced tremendous harm in power systems [24–26]. It is necessary to know the specific value of the relative position of the magnetic field at the maximum overvoltage and undervoltage as well as the law of the armature voltage distortion THD_U. Through magnetic field state analysis, the specific value of the relative position of the magnetic field at maximum overvoltage and undervoltage is also presented in this paper. With the asymmetrical current degree increasing, the law of the armature voltage distortion THD_U is calculated with the finite element method. This paper takes a nonsalient pole synchronous generator as an example, and we execute a two-dimensional finite element numerical computation. The result of the numerical computation is compared to the result of the analytic algorithm to verify the correctness of the analytic method. At the same time, several beneficial conclusions are reached.

2. Analysis of minor asymmetry and relative position of the magnetic field

2.1. Definition of minor asymmetry

Under asymmetric operation, the running states of the generator can be divided into fault and nonfault conditions. Generally, a minor asymmetric state of the generator, namely the nonfault unbalance condition, is decided by three factors. First, the negative current is below 8% of the rated current. Second, the deviation between the positive current and the rated current is below 10% of the rated current. Finally, the phase deviation between the positive current and the rated current is below 5 electrical angular degrees. This is shown in Eq. (1):

$$\begin{cases} \frac{I_2}{I_N} \leq 8\% \\ \frac{|I_1 - I_N|}{I_N} \leq 10\% \\ |\varphi - \varphi_n| \leq 5^\circ \end{cases} \tag{1}$$

Here, I_2 is the effective value of the negative current, I_1 is the effective value of the positive current, I_N is the effective value of the rated current, φ is the power factor angle of the positive network, and φ_n is the rated power factor angle of the positive sequence network.

2.2. Analysis of the relative position of the magnetic field

2.2.1. Analysis in symmetrical state

When the three-phase nonsalient synchronous generator operating under symmetrical state and A phase current is at maximum, instantaneous magneto-motive force vectors can be viewed as in Figure 1.

Here, $F'_{A1}, F'_{B1}, F'_{C1}$ is the positive magneto-motive force induced by the positive current of phase A, phase B, and phase C, and $F''_{A1}, F''_{B1}, F''_{C1}$ is the negative magneto-motive force induced by the positive sequence current of phase A, phase B, and phase C. According to the relationships between the positive and negative

magneto-motive force, they can be given by:

$$\begin{cases} F'_{A1} = F'_{B1} = F'_{C1} = F''_{A1} = F''_{B1} = F''_{C1} \\ \sum\limits_{i=A1,B1,C1} F_i = \sum\limits_{i=A1,B1,C1} F'_i = \frac{3}{2} F\phi 1 \cos(\beta - \omega t) \\ = \frac{3}{2}\frac{4}{\pi}\frac{\sqrt{2}}{2}\frac{Nkdp1}{p} I_1 \cos(\beta - \omega t) \\ \sum\limits_{i=A1,B1,C1} \vec{F''}_i = 0 \end{cases} \tag{2}$$

Here, $F\phi 1$ is the phase-fundamental magneto-motive force of the positive sequence, $p$is the number of pole pairs, and β, displayed in Figure 2, is the electrical angle between the winding axis of phase A and the complex magnetic field produced by the positive currents.

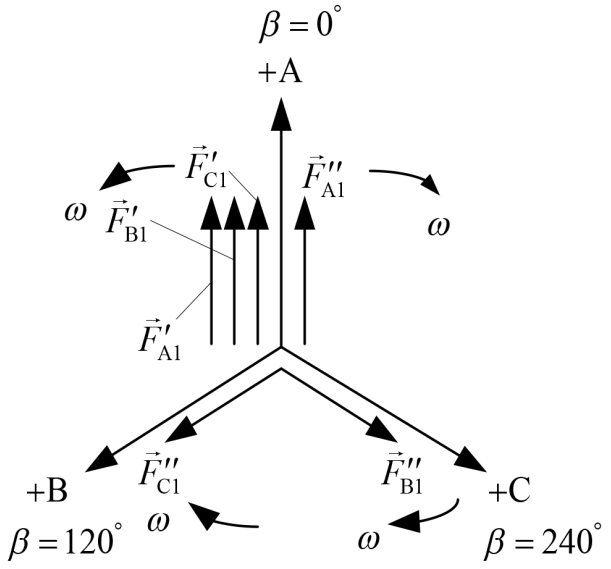

Figure 1. Magneto-motive force vectors under symmetrical operation when A phase current is at maximum.

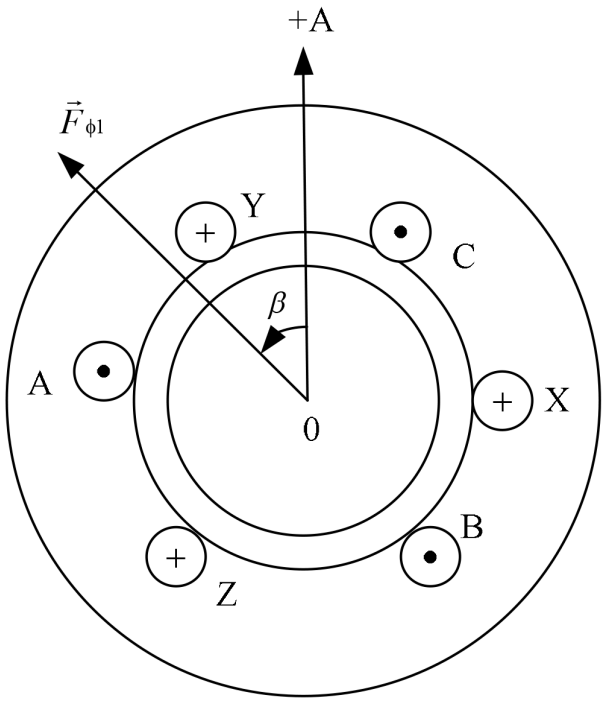

Figure 2. Spatial location of β.

2.2.2. Analysis under asymmetry state

When the current of phase A is at maximum, the angle between the complex positive magneto-motive force and the complex negative magneto-motive force is regarded as the relative position of the magnetic field, which is the angle between the positive and negative magnetic fields. This is illustrated in Figure 3 by χ.

The relationships between the positive and negative magnetic field amplitudes can be described by:

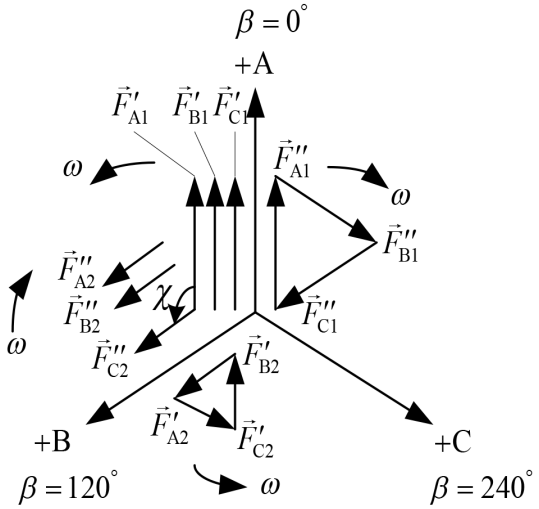

Figure 3. Magneto-motive force vector under asymmetrical operation when the relative position of the magnetic field is χ.

$$\begin{cases} F'_{A1} = F'_{B1} = F'_{C1} = F''_{A1} = F''_{B1} = F''_{C1} \\ \sum\limits_{i=A1,B1,C1} F_i = \sum\limits_{i=A1,B1,C1} F'_i = \frac{3}{2} F\phi 1 \cos(\beta - \omega t) \\ = \frac{3}{2}\frac{4}{\pi}\frac{\sqrt{2}}{2}\frac{Nkdp1}{p} I_1 \cos(\beta - \omega t) \\ F'_{A2} = F'_{B2} = F'_{C2} = F''_{A2} = F''_{B2} = F''_{C2} \\ \sum\limits_{i=A2,B2,C2} F_i = \sum\limits_{i=A2,B2,C2} F''_i = \frac{3}{2} F\phi 2 \cos(\chi + \beta + \omega t) \\ = \frac{3}{2}\frac{4}{\pi}\frac{\sqrt{2}}{2}\frac{Nkdp1}{p} I_2 \cos(\chi + \beta + \omega t) \\ \sum\limits_{i=A1,B1,C1} \vec{F''}_i = \sum\limits_{i=A2,B2,C2} \vec{F'}_i = 0 \end{cases} \tag{3}$$

Here, $F'_{A2}, F'_{B2}, F'_{C2}$ is the positive magneto-motive force induced by the negative current of phase A, phase B, and phase C, and $F''_{A2}, F''_{B2}, F''_{C2}$ is the negative magneto-motive force induced by the negative current of phase A, phase B, and phase C. I_2 is the effective value of the negative current and $F\phi 2$ is the phase-fundamental magneto-motive force of the negative sequence. χ' is the instantaneous angle between the complex positive magneto-motive force vector and the complex negative magneto-motive force vector, which changes over time.

3. Applying analytic method to analyze the influence of the relative position of the magnetic field on generator performance

3.1. Expressions of armature current

Define the asymmetrical degree of the current as $\alpha = I_2/I_1$. Based on the superposition formula of the same frequency sinusoidal quantity, the fundamental sinusoidal effective value of phase A can be given by:

$$g_A(\chi) = \sqrt{I_1^2 + I_2^2 + 2I_1 I_2 \cos(\chi)} \tag{4}$$

In order to simplify the process of derivation, make a variable substitution for Eq. (4) such that ζ equals $\cos(\chi)$. Hence, the function is exhibited as:

$$\begin{aligned} g_A(\zeta) &= \sqrt{I_1^2 + I_2^2 + 2I_1 I_2 \zeta} \\ &= \sqrt{I_1^2 + \alpha^2 I_1^2 + 2\alpha I_1^2 \zeta} = I_1 \sqrt{1 + \alpha^2 + 2\alpha\zeta} \end{aligned} \tag{5}$$

At the point of $\zeta_\omega = -\alpha/2$, the Taylor formula with Lagrange remainder term expansion in Eq. (5) can be shown by:

$$\begin{aligned} & g_A(\zeta)\Big|\alpha = \tfrac{I_2}{I_1} = I_1 + \tfrac{\alpha(\zeta+\frac{\alpha}{2})}{\sqrt{1+\alpha^2+2\alpha\zeta_\omega}} I_1 - \tfrac{\alpha^2(\zeta+\frac{\alpha}{2})^2}{2(1+\alpha^2+2\alpha\zeta')^{\frac{3}{2}}} I_1 \Big|\alpha = \tfrac{I_2}{I_1} \\ & = I_1 + \alpha(\zeta + \tfrac{\alpha}{2}) I_1 - \tfrac{1}{2} \tfrac{\alpha^2(\zeta+\frac{\alpha}{2})^2}{(1+\alpha^2+2\alpha\zeta')^{\frac{3}{2}}} I_1 \Big|\alpha = \tfrac{I_2}{I_1} \end{aligned} \tag{6}$$

Among them, the value of ζ' is between $-\alpha/2$ and ζ. Eq. (5) could be approximately represented by:

$$g_A(\zeta) I_1 + \alpha\zeta I_1 \tag{7}$$

As the asymmetrical degree grows smaller, the substitution of Eq. (7) for Eq. (5) will be more accurate. It is approximately shown as a sinusoidal function by the following:

$$\begin{bmatrix} I_A & I_B & I_C \end{bmatrix} \begin{bmatrix} I_1 & I_2 \end{bmatrix} \begin{bmatrix} 1 & 1 & 1 \\ \cos(\chi) & \cos(\chi + \frac{4}{3}\pi) & \cos(\chi - \frac{4}{3}\pi) \end{bmatrix} = I_1 \begin{bmatrix} 1 & \alpha \end{bmatrix} \begin{bmatrix} 1 & 1 & 1 \\ \cos(\chi) & \cos(\chi + \frac{4}{3}\pi) & \cos(\chi - \frac{4}{3}\pi) \end{bmatrix} \tag{8}$$

Apply Eq. (8) to compute the positive and negative currents such that I_1 and I_2 can be given by the following:

$$\begin{cases} I_1 = \frac{I_A + I_B + I_C}{3} \\ I_2 = \sqrt{\frac{I_A^2 + I_B^2 + I_C^2 - 3I_1^2}{3}} \end{cases} \tag{9}$$

3.2. Phasor expressions of armature voltage

Taking no account of the magnetic saturation, the rotating generator can be divided into three systems: the positive sequence system, negative sequence system, and zero sequence system. The parameters of the generator are shown in Table 1.

Assume $\gamma = R_1/R_\alpha$ and $\delta = X_1/X_\alpha$. R_1 is the external resistance of the positive sequence network, R_α is the rated resistance, X_1 is the external reactance of the positive sequence network, and X_α is the rated reactance. According to the relationships between the three sequence networks, the voltages can be displayed

Table 1. Design parameters of the generator.

Rated voltage/kV	24
Rated current/A	33,847
Power factor	0.9
Stator winding connection	Y
Per-phase resistance of the stator winding/Ω	0.00098
Negative sequence reactance (n on-saturation)/Ω	0.14165
Zero sequence reactance/Ω	0.07942

by:

$$\begin{cases} \dot{U}_A = \dot{I}_1 \left(\gamma R_\alpha + j\delta X_\alpha\right) + \theta \dot{I}_1 e^{j\chi} \left(R_2 + jX_2\right) \\ \dot{U}_B = \dot{I}_1 e^{-j120^0} \left(\gamma R_\alpha + j\delta X_\alpha\right) + \\ \theta \dot{I}_1 e^{j(\chi+120^0)} \left(R_2 + jX_2\right) \\ \dot{U}_C = \dot{I}_1 e^{j120^0} \left(\gamma R_\alpha + j\delta X_\alpha\right) + \\ \theta \dot{I}_1 e^{j(\chi-120^0)} \left(R_2 + jX_2\right) \end{cases} \tag{10}$$

Here, R_2 is the external resistance of the negative sequence network and X_2 is its external reactance. Assume the angle between the positive and negative sequence voltages of phase A, phase B, and phase C as ε_1, ε_2, and ε_3. The voltage of phases A–C is exhibited by:

$$\begin{cases} U_A = \sqrt{(U_1 + U_2\cos\varepsilon_1)^2 + (U_2\sin\varepsilon_1)^2} \\ U_B = \sqrt{(U_1 + U_2\cos\varepsilon_2)^2 + (U_2\sin\varepsilon_2)^2} \\ U_C = \sqrt{(U_1 + U_2\cos\varepsilon_3)^2 + (U_2\sin\varepsilon_3)^2} \end{cases} \tag{11}$$

Here, $\varepsilon_1 = \chi + \varsigma - \varphi$, $\varepsilon_2 = \chi + \varsigma - \varphi - 120^\circ$, $\varepsilon_3 = \chi + \varsigma - \varphi + 120^\circ$, U_1 is the effective value of the positive voltage, U_2 is the effective value of the negative voltage, and ς is the power factor of the negative sequence network. Providing Eqs. (10) and (11), we could achieve an angle between the maximum and minimum fundamental wave voltages of 180 electrical degrees in every phase. When the fundamental wave voltage of each phase is at its maximum, the corresponding χ_A, χ_B, χ_C are shown as:

$$\begin{cases} \chi_A = \varphi - \varsigma \\ \chi_B = \chi_A + 120^\circ; \chi_C = \chi_A - 120^\circ \end{cases} \tag{12}$$

4. Finite element simulation

4.1. Building the simulation model

When we build the model of the generator, the end effect of the magnetic field is ignored. In addition, current density J and magnetic vector potential A only have components along the generator axis direction. It is assumed that the axis direction is along axis Z. In the Cartesian coordinate system, current density J and magnetic vector potential A are the function of (x, y). To simplify the process of computation, the two-dimension finite model for the magnetic field, which is the round-section of the generator, is established. Assume the following:

1. The material of the generator is isotropic, the magnetic permeability of the stator core and the rotor core is constant, and the generator operates at unsaturated state.

2. Whereas the frequency of the generator is relatively low, the displacement current is so small that it compares with the conduction current. Hence, the impact of the displacement current can be neglected, namely $\frac{\partial D}{\partial t} = 0$.

3. The magnetic flux leakage does not exist outside the stator circle.

4. When the magnetic field changes or the temperature varies, resistance R keeps the same value, and the conditions in Eq. (13) below are satisfied in the solution domain of the generator's magnetic field.

$$\begin{cases} \Omega : \frac{\partial}{\partial x}\left(\gamma \frac{\partial AZ}{\partial x}\right) + \frac{\partial}{\partial y}\left(\gamma \frac{\partial AZ}{\partial y}\right) = -J_z \\ \Gamma : A_z = 0 \end{cases} \tag{13}$$

Here, γ is the magnetic reluctivity of the material, A_Z is the magnetic vector, and J_z is the current density. Ω is the complete solution domain of the generator's magnetic field. The physical model of the generator after subdivision and Ω are shown in Figure 4, and the magnetic field lines of the rated load are illustrated in Figure 5.

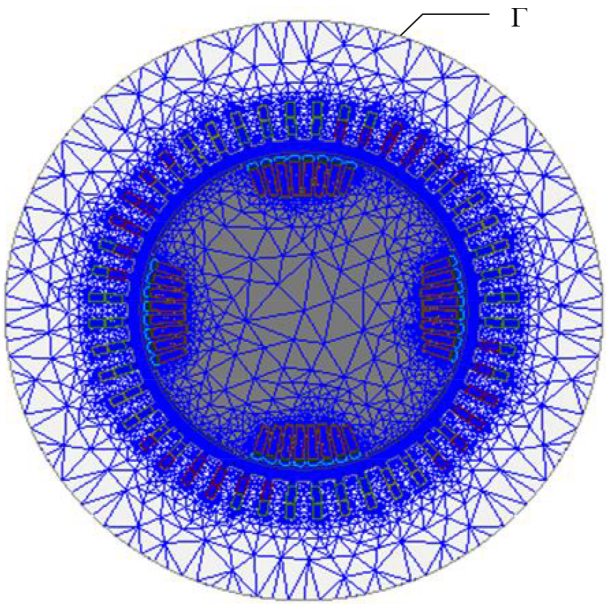

Figure 4. Physical model of the generator after subdivision.

The equivalent circuit diagram of the generator is displayed in Figure 6. By adjusting the impedance of phase A, phase B, and phase C, the asymmetrical degree α will be regulated.

Here, L_D is the reactance of the armature; L_δ is the leakage reactance of the armature; R_A, R_B, and R_C are the load-resistance of phases A, B, and C, respectively; and L_A, L_B, and L_C are the load-reactance of phases A, B, and C, respectively.

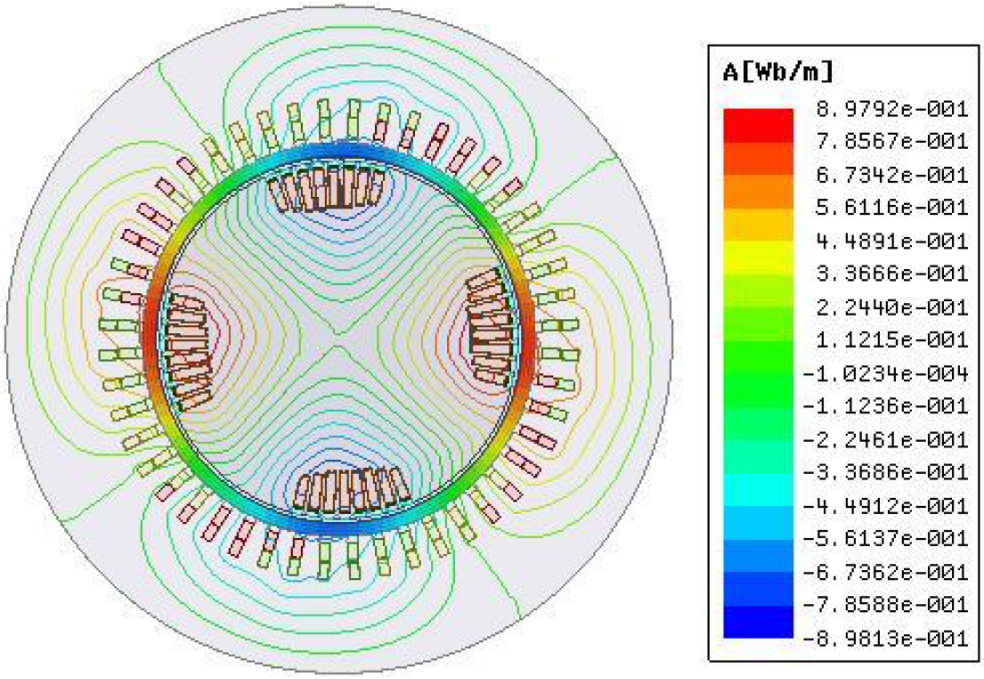

Figure 5. Magnetic field lines of the rated load.

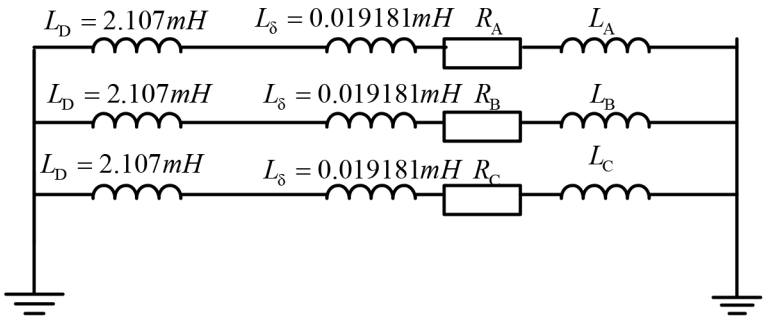

Figure 6. Equivalent circuit diagram of the generator.

When $\alpha = 1\%$, $\alpha = 2\%$, and 19%, the magnetic field flux density cloud map for the generator is as shown in Figure 7. The saturation characteristics of the stator and the rotor are shown in Figure 8.

4.2. Computation of armature currents through finite element simulation

The number of branches of the armature is two, namely $a_s = 2$.When the asymmetrical degree is 1%, 10%, 20%, and 50%, the simulation and analytic waves are displayed in Figures 9–12, respectively, which record the relationships between the armature current and the relative position of the magnetic field χ. The analytic waves are computed with Eq. (8).

Taking the analytic calculation method, the errors of the analytic method discussed in this paper and those of the traditional method are shown in Table 2. If the analytic Eq. (8) is employed, as the asymmetry increases, the error grows greater. When $\alpha \geq 6\%$, precision requirements in engineering will not be met. It transpires that when applying Eq. (9) to calculate I_1 and I_2, the effect of the minor asymmetrical degree is superior to that of the larger ones. At low asymmetrical degrees, the precision of the old method has

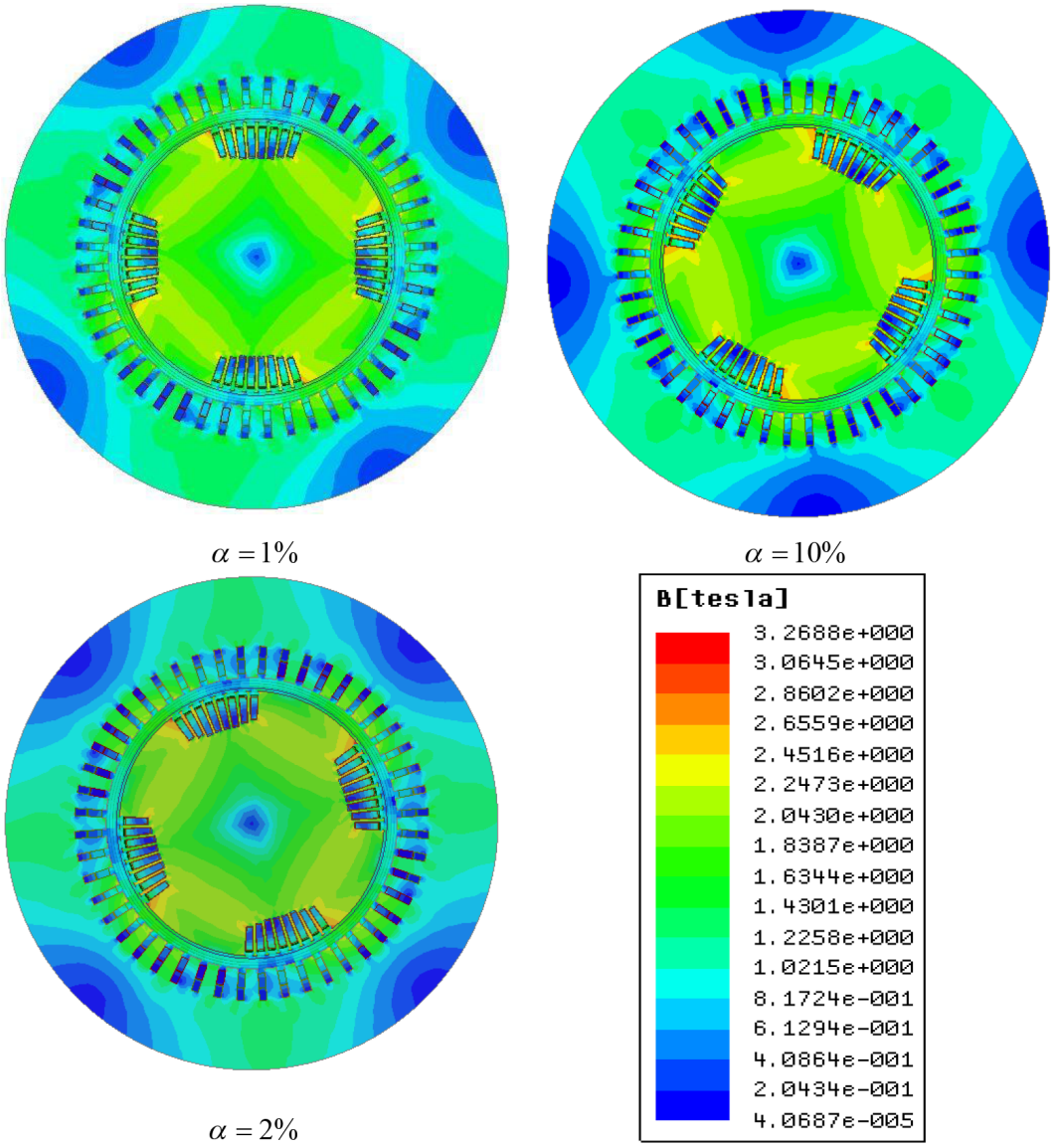

Figure 7. Magnetic field flux density cloud map for the generator.

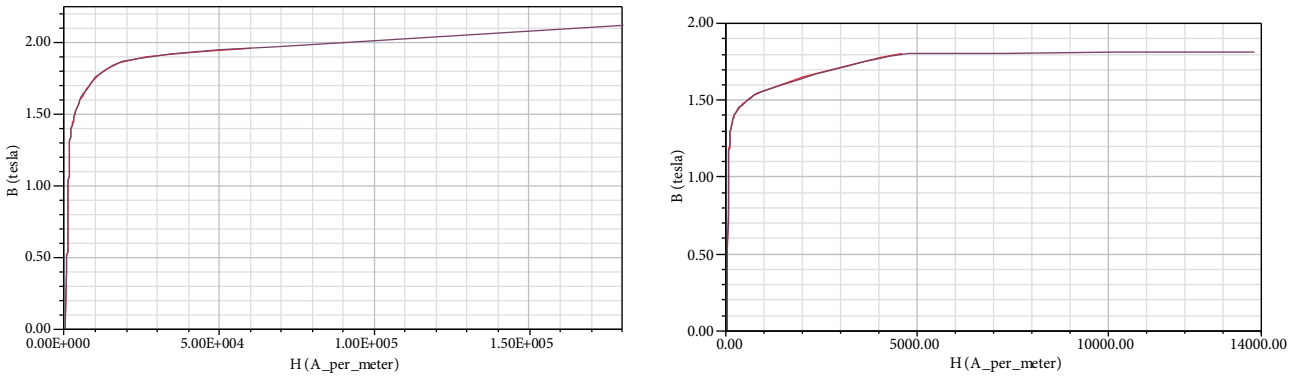

Figure 8. a) Stator saturation characteristics; b) rotor saturation characteristics.

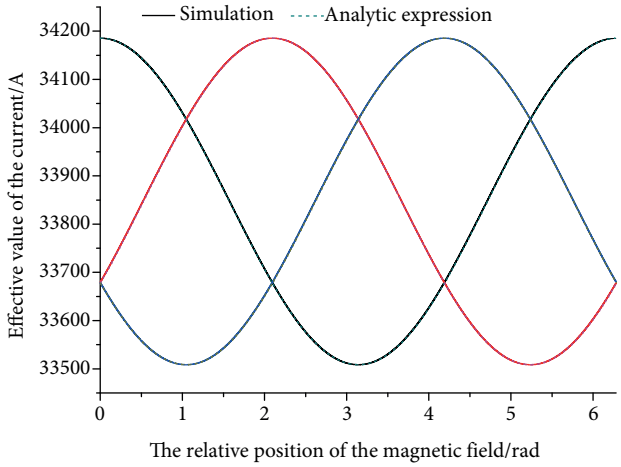

Figure 9. Curve of the current when the degree of asymmetry is 1%.

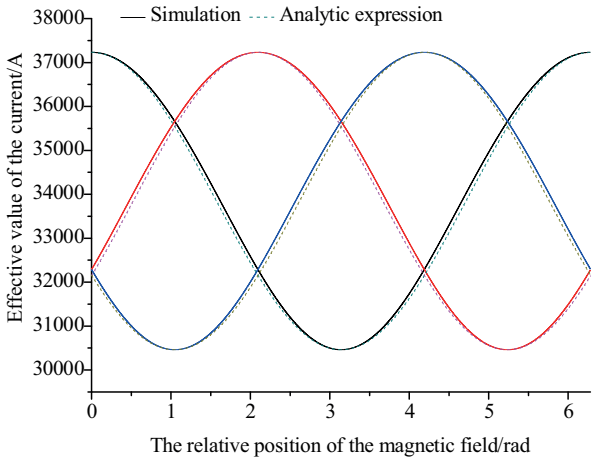

Figure 10. Curve of the current when the degree of asymmetry is 10%.

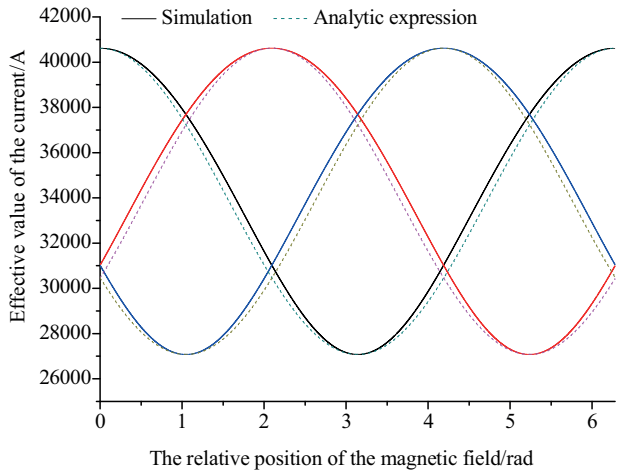

Figure 11. Curve of current when the degree of asymmetry is 20%.

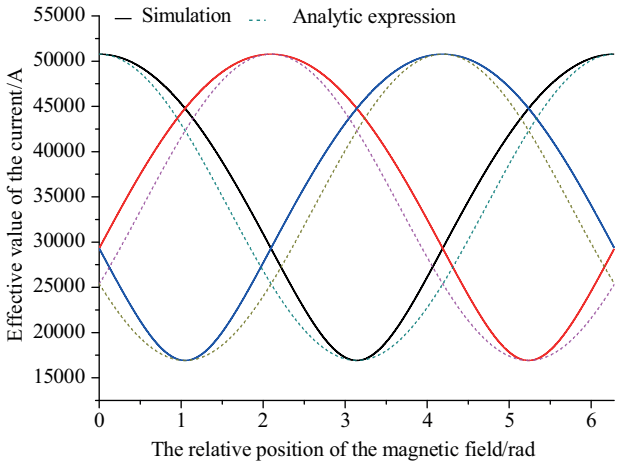

Figure 12. Curve of current when the degree of asymmetry is 50%.

superiority over that of the new method. However, the precision of the new method has superiority over that of the traditional method in high asymmetrical degrees. Relying on precision requirements in engineering, the effective range of this method is $\alpha \in [0, 6\%]$.

4.3. Computation of armature voltages through finite element simulation

Figures 13a and 13b show the maximum voltage $U\gamma_{MAX}$, calculated with the finite element method, when α is 1%, 2%, and 10% and the relative position of the magnetic field is $\chi = 0°, 30°, 60°, 90°, 120°, 150°, 180°, 210°, 240°, 270°, 300°$, and $330°$. Given that when the harmonic order is above 9, $U\gamma_{MAX}$ is very low and hence $\gamma > 9$; the harmonic waves are not shown in Figures 13a and 13b.

With the asymmetrical degree growing, as shown in Figures 13a and 13b, the voltage distortion U_D of the harmonic γ as well as the total voltage distortion THD_U present the gradual increment trend. When the generator is operating at a balanced state, α equals zero and $THD_U = 1.45\%$. Because of the increasing asymmetrical degree α, THD_U increases gradually. When α reaches 10%, $THD_U = 8.77\%$. Therefore, the

Table 2. Error of degree of asymmetry.

Asymmetrical degree (%)	Proposed method (A)	Traditional method (A)
1	1.6923×10^0	1.709×10^3
2	3.3847×10^2	1.726×10^3
3	6.7694×10^2	1.743×10^3
4	1.0154×10^3	1.76×10^3
5	1.3539×10^3	1.777×10^3
6	1.6923×10^3	1.794×10^3
7	2.0308×10^3	1.81×10^3
8	2.3693×10^3	1.827×10^3
10	3.0462×10^3	1.8416×10^3
20	6.4309×10^3	2.03×10^3
50	1.6585×10^4	2.538×10^3

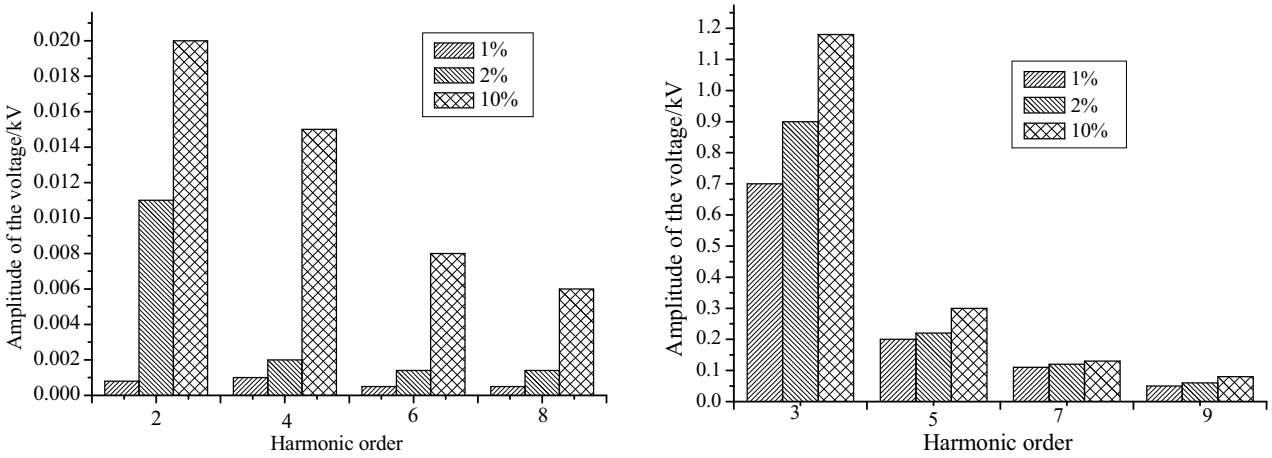

Figure 13. a) Even harmonic U$\gamma_{\max}$ when the degree of asymmetry is 1%, 2%, and 10%; b) odd harmonic U$\gamma_{\max}$ when the degree of asymmetry is 1%, 2%, and 10%.

influence of the harmonic voltage $\gamma \geq 2$ on the effective value can be ignored, especially at a minor asymmetrical degree. Therefore, the interference of the harmonic voltages $\gamma \geq 2$ can be neglected at the minor asymmetrical degree. It is feasible to use Eq. (11) to calculate the relative position of the magnetic field χ at maximum overvoltage and undervoltage. Supposing X = A, B, and C, we define the load coefficient of the generator as $\rho_x = r_x/R_\alpha$, and r_x is taken as the load resistance in the corresponding phase.

5. Conclusion

Based on the Lagrange analysis method, this paper proposes a new method to show the armature current. The result of the new analytic method is consistent with two-dimensional finite element numerical calculations.

The changing laws of the armature current and the armature voltage on the magnetic field state were analyzed. At minor asymmetrical degree of the current, with the alteration of the relative position of magnetic field χ, the current turns sinusoidal. With an increasing α, the voltage distortion U_D of the γ-order harmonic wave and total voltage distortion THD_U tend to increase gradually.

Relying on the Lagrange analysis and formula derivations, we exhibited a novel calculation method of the armature positive current I_1. The armature negative current I_2 and their effective ranges were also given.

The simulation of the two-dimensional finite element method verifies the correctness of the armature voltage phasor expressions that was deduced in this paper. When the generator runs at maximum overvoltage fault and maximum undervoltage fault, the three-phase relative positions of the magnetic field, namely, χ_A, χ_B, and χ_C, can be acquired by the positive sequence power factor angle φ and the negative sequence power factor angle ς, which is evidence of the generator's protection.

Acknowledgments

This project was supported by the National Natural Science Foundation of China (Project No: 51407050) and the National Science and Technology Major Project of China (Project No: 2009ZX060040).

References

[1] Diedrich C, Dijkstra D, Hamaekers J, Randrianarivony M. A finite element study on the effect of curvature on the reinforcement of matrices by randomly distributed and curved nanotubes. J Comput Theor Nanos 2015; 12: 2108-2116.

[2] Kumar R, Abbas I, Sharma V. A finite element study of unsteady free convection h- eat and mass transfer in a Walters B viscoelastic flow past a semi-infinite vertical plate. J Comput Theor Nanos 2014; 11: 2469-2475.

[3] Abbas IA, Singh B. Finite element analysis in a rotating thermoelastic half-space with diffusion. J Comput Theor Nanos 2014; 11: 2276-2282.

[4] Ning YH, Liu C, Zhu SH. Design and finite element analysis of a hybrid excitation synchronous machine. Int J Appl Electrom 2015; 48: 11-19.

[5] Kar N, Murata T, Tamura J. A new method to evaluate the q-axis saturation characteristic of cylindrical-rotor synchronous generators. IEEE T Energy Conver 2000; 15: 269-276.

[6] Kar NC, El Serafi AM. Measure of the saturation characteristics in the quadrature axis of synchronous machines. IEEE T Energy Conver 2006; 21: 690-698.

[7] Ge BJ, Li YL, Li B. Study of starting process of pumped storage machines by static frequency converter. Elect Mach Control 2002; 6: 95-99.

[8] Wang D, Wu XZ, Ma WM. Air-gap MMF analysis of fifteen-phase induction motor with non-sinusoidal supply. Proceedings of the CSEE 2009; 29: 88-94.

[9] Xing JQ, Wang FX, Wang TY. Study on anti-demagnetization of magnet for high speed permanent magnet machine. IEEE T Appl Supercon 2010; 20: 856-860.

[10] Kang GH, Hur J, Nam H. Analysis of irreversible magnet demagnetization in line-start motors based on the finite-element method. IEEE T Magnetics 2003; 39: 1488-1491.

[11] Liang YP, Huang H, Li LH. Numerical calculation of end region of large air-cooled turbogenerator. Proceedings of the CSEE 2007; 27: 73-77.

[12] Huang H, Feng JQ, Liang YP. Numerical calculation of stator end-leakage of large air-cooled turbo-generator. Large Electric Machine and Hydraulic Turbine 2006; 20-23 (in Chinese).

[13] Liu XF, Meng L, Luo YL. The saturation curve series of synchronous generators. Proceedings of the CSEE 2002; 22: 68-72.

[14] Li LY, Pan DH, Huang XZ. Analysis and optimization of ironless permanent-magnet linear motor for improving thrust. IEEE T Plasma Sci 2013; 41: 1188-1192.

[15] Pollard EI. Effects of negative-sequence currents on turbine-generator rotors. T Am Inst Electr Eng 1953; 72: 404-406.

[16] Zhang ZY, Ma HZ, Zhong Q, Zhao LJ. Negative sequence component characteristics analysis of PMSM under asymmetry operation condition. Electr Meas Inst 2014; 51: 46-50.

[17] Jiang T, Guo ZZ, Chen XY, Xue F. Fault analysis of polymorphic phase component in electric power system and the application in the asymmetry system. Proceedings of the CSEE 2005; 22: 70-74.

[18] Li WL, Sun JH, Sun HL. Calculation and analysis of eddy loss and temperature field in rotor of synchronous generator under steady state and negative sequence. T China Elec Soc 2012; 27: 174-182.

[19] Paithankar YG, Bhide SR. A fast method for sequence component filtering. Int J Elect Eng Educ 2003; 40: 66-71.

[20] Sengupta S, Mukhopadhyay AK. Development of microprocessor based negative phase sequence current monitoring unit and negative phase sequence relay for an AC generator. J Inst Eng 2001; 82: 220-226.

[21] Islam SM. Novel microprocessor based negative phase sequence relay and meter. Int J Elec Power 1996; 18: 547-552.

[22] Akagi H, Kanegauwa Y, Nabaes A. Instantaneous reactive power compensators comprising switch devices without energy storage components. IEEE T Ind Appl 1984; 20: 625-630.

[23] Takeda M, Ikeda K, Teramoto A. Harmonic current and reactive power compensation with an active filter. In: IEEE 1998 Power Electronics Specialists Conference; 11–14 April 1988; Kyoto, Japan. New York, NY, USA: IEEE. pp. 174-1179.

[24] Wang HW, Jiang WP, Wu YN. Study on last break trip fault of inverter station in 800 kV UHVDC project from Yunnan to Guangdong. Power Syst Technol 2008; 32: 6-9.

[25] Dong ML, Li XL, He JJ. Electromagnetic transient response characteristics of internal faults in UHVDC converter station and corresponding control strategy. Power Syst Technol 2010; 34: 5-10.

[26] Zhang BD, Luo B, Zhang JH. Generators merging network conditions accounting method based on the positive sequence fundamental voltage synthetic phasor. Proceedings of the CSEE 2006; 16: 52-56.